WORLD CONFERENCE ON TIMBER ENGINEERING 2025
BRISBANE, AUSTRALIA
Advancing Timber for the Future Built Environment

Fire safe design of hybrid steel-timber construction systems

Patrick Dumler[1], Jakob Blankenhagen[2], Martin Mensinger[3], Stefan Winter[4]

ABSTRACT: As part of the research project "BraStaHo" (Fire Safety of Hybrid Steel-Timber Construction Systems), two hybrid steel-timber construction systems were investigated under fire exposure using the standard fire curve. One objective was to assess the fire protection capacity of timber linings for steel beams over various time periods and identifying key factors influencing their effectiveness. As another objective, the project examined slim floor type construction systems with steel and timber elements. Experimental investigations provided valuable insights into the combustion behavior of these systems, with particular emphasis on support conditions and cavities, as these elements pose the highest risk for structural failure and smoke propagation. The deformation behaviour of the floor under fire exposure and mechanical load has also been analyzed, which showed an influence on the charring rate in the support area. Different methods to protect the steel beam from direct fire exposure and their influence on the thermal behaviour have been tested. The ultimate goal of these tests was to develop fire-safe support details and accurately predict the thermal response of slim-floor constructions in fire scenarios. The main findings for the slim floor tests are described in this paper.

KEYWORDS: timber, steel, hybrid, fire

1 – INTRODUCTION

A typical application of hybrid steel-timber constructions involves supporting timber floor elements on slender, wide-span steel girders. When supported on the lower flanges, the overall height of the ceiling structure can be reduced, creating a "slim floor" design. Another option is to clad linear steel elements (columns/beams) with solid wood panels, protecting the internal load-bearing components from thermal stress in the event of a fire. However, hybrid steel-timber construction has not yet been widely adopted in practice due to gaps in knowledge and scepticism regarding its fire safety. The findings and results on the thermal behaviour of these two systems, obtained through experimental investigations as part of the ongoing research project "BraStaHo" (Fire safety of hybrid steel-timber construction systems), will be presented.

2 – EXPERIMENTAL SETUP

Building on the first validation test [1], a total of seven test specimens were evaluated for the slim floor construction to assess several construction variants. All tests were conducted in the same fire furnace as the validation test, with internal dimensions of 3.0 m × 1.0 m × 1.5 m. The fire exposure followed the standard fire curve (SFC).

Each floor test specimen consisted of two HEB300 and two UPE300 profiles, each 1.2 m long. Three Cross Laminated Timber (CLT) elements, each 160 mm thick and 750 mm wide, were placed on the bottom flanges of the beams. The fire-exposed length of the elements was 1.0 m (see Fig. 1). The test specimens had an average wood moisture content of 11.6 % with a relative standard deviation of 4.3 %. The specimens differed in several aspects to evaluate the various factors influencing the charring behavior.

One key variation was the lining of the beams. For six of the test specimens, the lining was deliberately omitted to shorten the test duration and allow for a faster charring of the system. In one configuration, the beam was coated with a reactive fire protection system in the form of an intumescent paint. An alternate specimen featured a 22 mm thick three-layer timber board as lining.

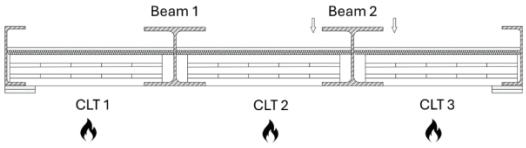

Figure 1: Schematic setup of a floor specimen with mechanical loading on beam 2

[1] Patrick Dumler, Chair of Timber Structures and Building Construction, Technical University of Munich, Munich, Germany, patrick.dumler@tum.de , ORCID: 0009-0009-9498-1674

[2] Jakob Blankenhagen, Chair of Metal Structures, Technical University of Munich, Munich, Germany, jakob.blankenhagen@tum.de , ORCID: 0000-0001-6954-6421

[3] Martin Mensinger, Chair of Metal Structures, Technical University of Munich, Munich, Germany, mensinger@tum.de , ORCID: 0000-0001-5210-5400

[4] Stefan Winter, Chair of Timber Structures and Building Construction, Technical University of Munich, Munich, Germany, winter@tum.de , ORCID: 0000-0002-5825-0710

https://doi.org/10.52202/080513-0449

Another factor examined was the support backing beneath the CLT elements. No backing was used in two specimens, whereas in four alternate specimens, a layer of gypsum plasterboard was placed under the CLT element at the support. In an additional variation, an extra gypsum plasterboard panel was installed to cover the narrow side of the CLT element.

The influence of element joints in the CLT elements was also investigated. Some test specimens had no joints, while others included an element joint covered by a top board to assess its impact on fire resistance.

Furthermore, the cavity between the steel beam and the CLT element was examined in different configurations. This cavity remained empty in one test, while in the other tests, it was filled with either mineral wool or perlite granulate to evaluate their effectiveness in fire protection.

Finally, the influence of mechanical loading on the floor system was considered. One side of the specimen was tested without any mechanical load. In contrast, on the other side, the supported CLT elements were subjected to a load of 10 kN/m in the support area to assess the structural response under fire exposure.

Fig. 2 shows the view of one specimen after placing it on the furnace, while Table 1 gives an overview of the testing setup.

3 – TESTING PROCEDURE

The test was conducted in a three step procedure. First, the mechanical load was applied, then the burner was ignited. Finally, the specimen was removed from the furnace to extinguish it. The time interval between removal from the furnace and the start of the extinguishing process was recorded and considered when calculating the charring rate based on the remaining cross-section. Additionally, in selected tests, the temperature development during the extinguishing process was measured to evaluate the efficiency of the extinguishing method.

The temperature measurement was conducted using Type K thermocouples (see Fig. 3). The measurement points were positioned at the web (x_1 and x_2), 3 cm in the CLT element (x_3 and x_4), 1cm in the CLT element (x_5 and x_6), in the support area of the CLT element (x_7 and x_8), as well as at the bottom flange of the steel beams (x_9, x_10, x_11 and x_12).

Figure 2: View of the specimen on the furnace without encapsulation from the outside

Table 1: Overview of test setup

Specimen	Protection	Joint	Support	Cavity
SP1 left	22 mm Timber	-	-	Perlite
SP1 right	Coating	-	- / Gypsum 12.5 mm	Mineral wool
SP2	-	-	-	-
SP3	-	Top board	-	Mineral wool
SP4	-	Top board	Gypsum 12.5 mm	Mineral wool
SP5	-	-	Gypsum 18 mm	Mineral wool
SP6	-	-	Gypsum 18 mm	Mineral wool
SP7	-	-	Gypsum 12.5 mm	Mineral wool

The furnace temperature was also measured at the steel beams' exposed surface on two levels using sheathed thermocouples, which were used as thermal load for the numerical simulations.

The temperature was controlled via two centrally positioned plate thermocouples, which were placed along the beam length at the center and at a distance of 10 cm from the two beam surfaces.

The tests were terminated at different time points. One termination criterion was reaching the predefined critical temperature limit of 500 °C at the web or bottom flange of a steel beam. Another criterion was the deformation of the mechanically loaded beam, as the hydraulic cylinders eventually reached their maximum extension length, preventing further load application.

4 – RESULTS

4.1 TEMPERATURE

Lining and reactive fire protection system

The influence of the investigated variants was compared based on their temperature profiles.

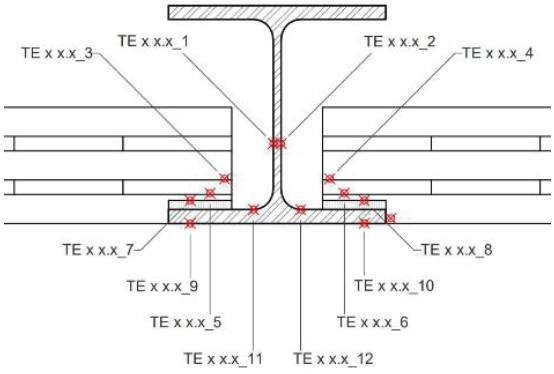

Figure 3: Measurement points for one layer of a steal beam

https://doi.org/10.52202/080513-0449

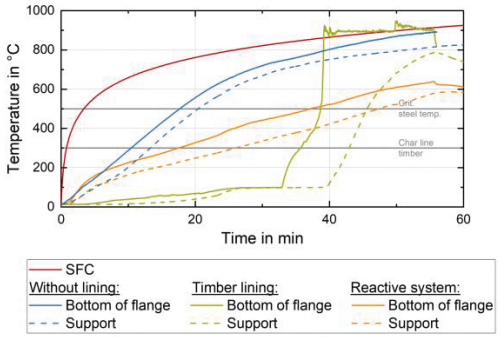

Figure 4: Temperature profiles for different protection systems

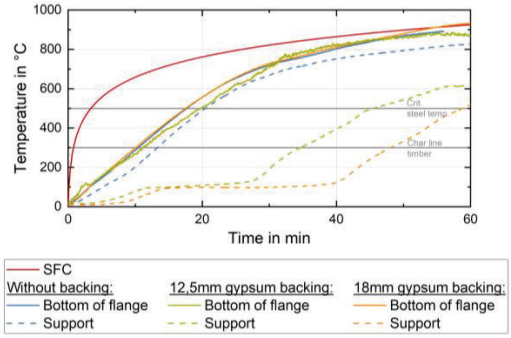

Figure 5: Temperature profiles for different backing thicknesses

In Fig. 4, a distinction can be made between an unprotected beam (blue), a protected beam with a 22 mm thick three-layer timber board (green), and a beam with an intumescent fire protection coating (orange). For comparison purposes, the SFC is shown in red.

The unprotected beam exhibits a rapid temperature increase, reaching the charring line of timber on its underside after approximately 10 minutes. The heat penetration through the bottom flange takes another three minutes, meaning that ignition of the CLT in the support area is expected after 13 minutes. The critical steel temperature of 500 °C is exceeded for the flange after about 18 minutes.

In comparison, the beam with fire protection lining shows significant differences in its temperature curves. The bottom side forms a plateau at 100 °C after approximately 25 minutes. This temperature level is maintained for six minutes until all bound water in the timber evaporates. After this phase, a sudden temperature rise occurs as the lining deteriorates due to advanced charring and falling off. The designated fire protection duration of 30 minutes is reached.

For the beam with an intumescent fire protection coating, the initial temperature rise is similar to that of the unprotected beam. However, at around 200 °C, the temperature curves begin to flatten. This indicates the expansion and beginning of isolation for the steel beam from thermal exposure. As a result, the char line of timber is reached later, at approximately 25 minutes, on the top side of the bottom flange.

Overall, both fire protection systems effectively reduce the temperature increase. However, the timber lining maintains temperatures below 100 °C for an extended period. Once the lining deteriorates, a sudden temperature rise occurs because the beam is unprotected in an environment exposed to high temperatures. In contrast, the intumescent coating gradually reduces the rise of the beam's temperature once it expands. However, since this system is specifically designed for steel, the 300 °C isotherm in the support area is exceeded earlier than with the timber lining, leading to an earlier onset of charring in the CLT element.

CLT Backing

The following test specimens differed in the support area due to adding gypsum fiberboards beneath the CLT element, with thicknesses of 12.5 mm (green) and 18 mm (orange). The solid lines in Fig. 5 represent measurement points at the fire-exposed side of the bottom flange, where all three test specimens were tested without any fire protection system. The temperature curves show a similar pattern, indicating that the additional support layer does not influence the heating behaviour of the bottom flange.

The dashed lines represent the temperature between the CLT element and the steel beam or between the CLT element and the support layer. When the CLT is placed directly on the beam without an additional layer, the char line of wood is exceeded after just 13 minutes. The heat transfer from the bottom to the top side of the bottom flange takes approximately three minutes.

In contrast, the temperature increase on the underside of the CLT element is significantly delayed for the two test specimens with a backing. A temperature plateau forms at 100 °C, which is maintained for 15 minutes with the 12.5 mm board and for 25 minutes with the 18 mm board. After the bound water in the gypsum has evaporated, the temperature begins to rise again. However, compared to timber-based fire protection lining (as shown in Fig. 4), this increase is less abrupt, as the backing layer remains in place and does not detach, preventing direct exposure of the surface. Despite the exposed steel beam, the selected support layer significantly delays the onset of wood charring. Compared to the unprotected variant, the time required to exceed the 300 °C isotherm is extended by 21 minutes and 35 minutes, respectively.

Cavity filling

In Fig. 6, the blue curves represent the test specimen with an air-filled cavity. The green curves represent a specimen where the cavity was filled with mineral wool insulation. In contrast, the orange lines also featured an additional lining of the narrow side of the CLT element with gypsum fiberboard panels. The comparison focuses on three measurement points: the bottom side of the flange, the transition between the CLT element and the steel beam (or between the CLT element and the backing layer) and the beam's web.

https://doi.org/10.52202/080513-0449

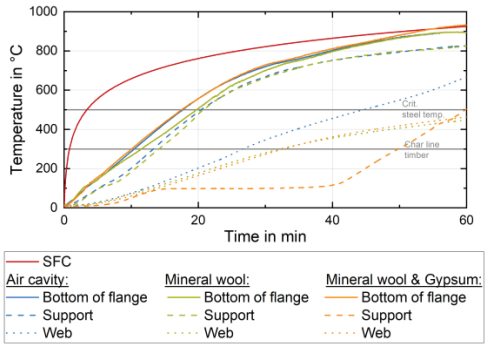

Figure 6: Temperature profiles for different cavity designs

The unprotected bottom flange shows a similar temperature increase for all three test specimens, exceeding the critical steel temperature after an average of 19 minutes. The mineral wool insulation does not provide a noticeable protective effect in the support area. The 300 °C isotherm is reached after approximately 20 minutes for both specimens with the unprotected cavity and the cavity filled with mineral wool, but without additional backing at the support.

In contrast, the protective effect of the backing layer is clearly visible, as it creates a temperature plateau at 100 °C for 25 minutes. The temperature development in the steel web varies depending on the cavity insulation.

The char line and the critical steel temperature are reached earlier for the uninsulated test specimen. The mineral wool insulation reduces heat transfer by blocking radiative exchange between surfaces and convective heat transfer within the cavity. Since charring of the CLT element can be expected from minute 13 onward, the cavity insulation protects the steel web from the resulting thermal exposure.

For the insulated test specimens, it can therefore be assumed that the temperature increase is primarily due to heat conduction. This is confirmed by the test specimen with the additional narrow-side lining, where charring of the CLT element does not begin until minute 50. At the same time, the temperature development in the steel web remains similar to that of the test specimen with just mineral wool insulation.

The cavity filling and the narrow-side lining showed positive effects, leading to improved charring behaviour in the support area. On the one hand, the cavity filling prevents heat exchange within the cavity, and on the other hand, the lining protects the CLT element from charring. As a result, the onset of charring is significantly delayed. Additionally, the narrow-side lining prevents the fire from spreading around the corner along the narrow side of the CLT element.

Element joints

The temperature curves, as well as the visual of the burned specimens, yielded a similar result. The executed element joint, consisting of a top board, adhesive tape sealing, and a joint width of 2 mm, has no noticeable effect on the charring behaviour of the CLT element. Therefore, with a typical construction of element joints in practical applications, no increased charring is expected for steel-timber hybrid floors.

4.2 CHARRING

The CLT elements were divided into two measurement areas to determine the charring rate. One area focused on the support region, while the other examined the freely exposed surface between the steel beams. The charring depth was measured using two methods. First, 3D scans of the test specimens were conducted using Autodesk Recap. Afterwards, a manual measurement was used.

To determine the charring rate, the time points at which the charring of the CLT element in the support area began were first identified. This condition was considered met when the 300 °C isotherm was recorded on the bottom side of the CLT element. The fire exposure duration was calculated based on the start of charring and the beginning of the extinguishing process. Since no further exposure to the STC occurred between turning off the burners and the start of extinguishing, it was assumed that the charring rate decreased during this period. Therefore, the total fire exposure duration was reduced by 20 % for this phase. The charring rate, expressed in millimetres per minute, was then determined by dividing the measured charring depth of the test specimens by the effective fire exposure duration.

The results indicate that the charring rate under the applied mechanical loading was 25 - 27 % higher than the unloaded element. This increase is attributed to the compression of the charcoal layer under load, which reduces its insulating effect and leads to a faster charring process. The measured charring rate on the freely exposed surface was similar to the one-dimensional charring rate β_0 = 0.65 mm/min specified in [2]. In contrast, a lower charring rate was observed in the unloaded support area. This reduction is due to the shielding effect of the steel beam's bottom flange, which limits heat transfer by preventing free convection. The steel absorbs part of the heat and dissipates it through its high thermal conductivity via the web.

For the loaded support area, the opposing effects of shielding and compression of the charcoal layer seem to partially cancel each other out, resulting in a charring rate similar to that of the freely exposed surface of the CLT element.

The intumescent fire protection coating reduced the measured charring rate to 0.40 – 0.48 mm/min due to the insulating effect of the expanded material. While the charring process was not completely prevented - since the temperatures at the beam exceeded the 300 °C isotherm - the overall heat input into the steel was lower. This reduced the thermal load compared to an unprotected beam, leading to a lower charring rate. The different charring rates depending on the measurement method and the considered area of the specimen, respectively its construction, are given in Table 2.

https://doi.org/10.52202/080513-0449

Table 2: Charring rate of the different areas of a specimen depending on the measurement method

	Charring rate [mm/min]	
	3D-Scan	*Manual Measurement*
CLT surface	0.68	0.68
Support unloaded	0.54	0.51
Support loaded	0.69	0.64
Support with coating	0.48	0.40

4.3 EXTINGUISHING

After the furnace burners were turned off, the test specimens were lifted from the furnace and subsequently extinguished with water. The extinguishing process initially focused on the bottom side of the floor specimens. Afterwards, the upper structure was removed, exposing the CLT elements. It was observed that even after extinguishing the bottom side, temperatures within the construction remained above 100 °C. On the one hand, water evaporated from the steel beam, forming bubbles, and the surface dried quickly. On the other hand, after opening the test specimen, open flames and glowing embers were still present in the support area (see Fig. 7).

Some specimen's temperatures were still recorded after the burners were turned off. The measurements clearly show that an extinguishing attack from below is ineffective due to the construction design, making it challenging to reach ongoing charring in the support area. Since the extinguishing water cannot penetrate the construction, immediate suppression of the affected areas is not possible. An extinguishing attack from above is also not feasible in a typical floor construction.

The extinguishing behaviour largely depends on the depth of the affected layers and the fire's progression. In near-surface areas, faster cooling was observed, such as on the directly exposed bottom flange, where temperatures dropped immediately after the burners were turned off. However, in the support area, fire can persist despite the extinguishing attempt due to limited accessibility, potentially leading to a continued temperature increase (see Fig. 8).

A suitable structural design should be implemented to prevent charring in the support area from the outset. This would help minimise the fire risk and the associated challenges in fire suppression.

Figure 7: Temperature profiles after turning off of the furnace

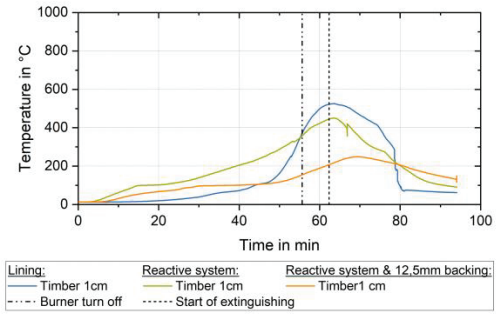

Figure 8: Temperature profiles after turning off the furnace

4.4 DEFORMATION

The mechanical loading on beam 2 of the individual floor specimens was examined to determine its influence on the charring behaviour of the wood. It has already been demonstrated that the protective effect of the charcoal layer is partially reduced by the applied load, leading to an increased charring rate. Displacement sensors were installed on the two loaded CLT elements to measure the deformation of the charcoal layer and the CLT element.

The unprotected test specimen reached the charring threshold in the support area after approximately 13 minutes, marking the onset of charring (see Fig. 9). no significant deformation was yet measurable. A minimal increase in deformation was observed after 11 minutes, which can be attributed to shrinkage effects in the wood as well as deformation of the steel flange. Once the charring threshold was reached, the formation of the charcoal layer led to a more pronounced increase in deformation, which progressed almost linearly from minute 25 onward. The deformation increased to 22 mm, at which point the hydraulic system was fully extended. This resulted in a sudden loss of force, making further adjustments impossible, and the test had to be terminated. The linear increase corresponds to a deformation rate of approximately 0.38 mm/min.

The deformation observed during the test was also clearly visible (see Fig. 10). Due to the progressive compression in the support area, the test specimens tilted toward the loaded beam.

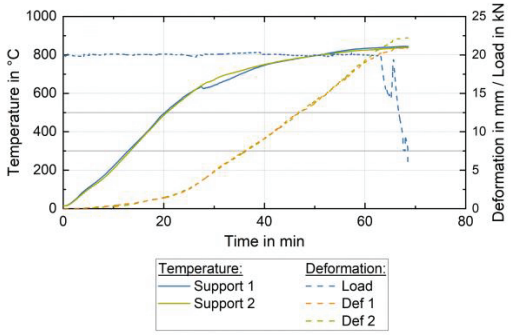

Figure 9: Temperature and deformation curves for loaded CLT elements

https://doi.org/10.52202/080513-0449

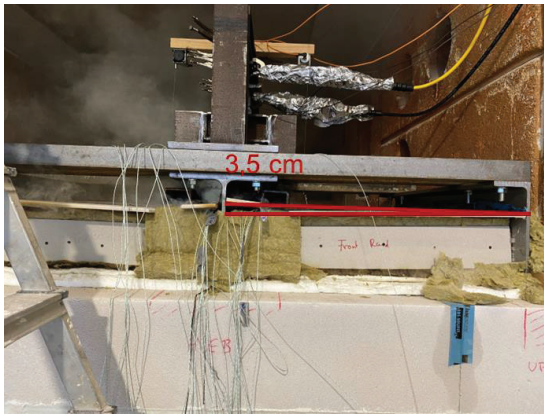

Figure 10: Deformation of the specimen during the test

After the test, the difference in the height of the charcoal layer was particularly evident when the test specimens were opened. This suggests that under normal service loads, significant deformations of the floor can be expected if a fire occurs in the support area.

Such large-scale deformations of the floor can significantly impact fire-protected components' required fire resistance duration. Furthermore, they can lead to structural problems, as these deformations are typically not considered in the structure's design.

It is, therefore, essential to consider the potential effects of fires in the support area during planning and design and to implement appropriate measures to prevent charring at the support.

The uniform deformation curve suggests that the stepwise charring model from [3] does not apply to the support region. This model assumes that once a protective lining fails (t_f), an increased charring rate occurs due to the loss of the protective charcoal layer and the intensified thermal exposure from the developed fire. The charring rate would decrease once a sufficiently thick charcoal layer has formed. However, in the tested floors a detachment of protective layers or coal is not possible. Additionally, the steel beam's flange provided additional shielding.

5 – NUMERICAL SIMULATION

5.1 MODEL

A thermal-transient modelling approach was used to simulate the floor systems. The generated temperature field was used to extract the temperature development at specific measurement points from the test specimen setups. The primary objective was to assess how well the thermal behaviour of the considered cross-sections, including radiation in cavities, the use of gypsum fiberboard backing layers, and the behaviour of intumescent coatings, can be predicted using numerical models.

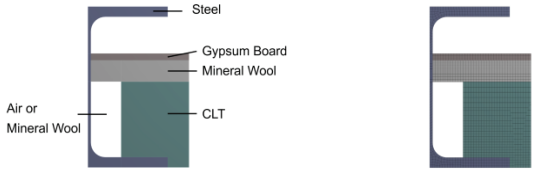

Figure 11: Model of the floor specimen with an air-filled cavity (right: with mesh)

The individual floor specimens were created using the Design Modeler integrated into Ansys Workbench. The heat transfer in the test specimens was considered exclusively perpendicular to the layers (from the fire-exposed side towards the unexposed side). A three-dimensional model with a depth of 5 mm was used to simulate radiative heat exchange within cavities. A symmetry plane was applied to both the steel profile and the CLT element to reduce computational time. The CLT element was extended 40 mm beyond the bottom flange's outer edge to minimise charring's influence in the support area. Additionally, a sensitivity analysis was performed to determine the optimal mesh size. Based on the results, the element size for the floor model was set to 5 mm (see Fig. 11).

Automated contact conditions of the "bonded" type were used to calculate the temperature distribution at the interfaces. In cases of full contact, these conditions allowed unrestricted heat flow. The air cavities were modelled just using surface-to-surface radiation. Transitions were assumed to be perfect, meaning no heat losses occurred within the model.

Since the air temperature in the furnace near the steel beams was relatively homogeneous and uniform, the average temperature of the four measurement points from the sheathed thermocouples was used as the thermal load for the numerical model. The thermal load was applied in the form of radiation and convection. The unexposed side of each floor was loaded with the ambient temperature present during the test. On the fire-exposed side, a heat transfer coefficient of 25 W/m²K [4] was applied, while the unexposed side was subjected to a coefficient of 4 W/m²K [4]. Emissivity was incorporated based on material-specific emissivity values: 0.7 for steel [5], 0.9 for gypsum fiberboard [6] and intumescent coating [7], and 0.8 for other materials [3].

The material properties of steel, as described in [5], were used. For timber, the values of [3] were applied. For mineral wool, the values were based on [6]. Since no specific density from the data sheet was provided, it was set at 40 kg/m³. The specific heat capacity of gypsum boards varies significantly in the literature [6, 8, 9]. For the simulation, the experimentally calibrated value for gypsum fiberboard from [6] was used, as it provided the best agreement with the experimental results in a parameter study. The density of 800 kg/m³ at 20 °C was taken from the datasheet. The density of the intumescent fire protection coating was set to a constant value of 100 kg/m³, based on [10]. The specific heat capacity was also assumed to be constant, with a value of 1200 J/kgK [11].

https://doi.org/10.52202/080513-0449

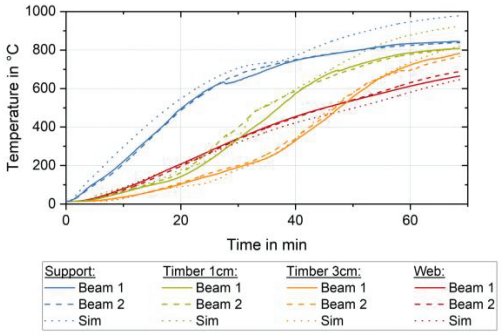

Figure 12: Comparison of simulation and results for air-filled cavity

The thermal conductivity was modelled as temperature-dependent, ranging from 0.3 W/mK to 0.05 W/mK, based on the data from [7]. The optimal coating thickness was determined through a parameter study, with the best results obtained for a thickness of 1.2 mm.

5.2 RESULTS

The simulated graphs are shown as dotted lines in Fig. 12 - Fig. 15, while solid or dashed curves represent the measured values. A total of four specific measurement locations were compared.

The diagram for the specimen with an air-filled cavity indicates that the numerically determined temperatures at the support and in the CLT element at a depth of 1 cm are, on average, slightly higher (conservative) than the temperatures measured during the experiments (see Fig. 12). At the web, the temperatures are consistently underestimated after 30 minutes but remain within a similar range. The chosen approach to model the cavity using radiation without heat losses and the selected material parameters leads to results that align well with the fire tests overall. Some more significant deviations in the temperature curves can be observed for the integration of the backing layer and narrow-side lining. The simulation reproduces the plateau at 100 °C with the selected material parameters like the experimental results. The slopes of the graphs are at a comparable level. The simulation also captures the different timings of the subsequent temperature rise, depending on the board thickness, although the increase occurs slightly later. The numerical results at the support and CLT element are initially below the measured curves (see Fig. 13).

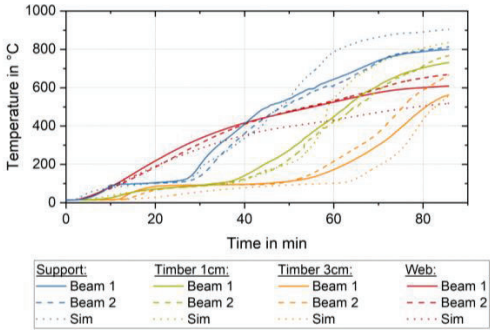

Figure 13: Comparison of simulation and results for 18 mm backing

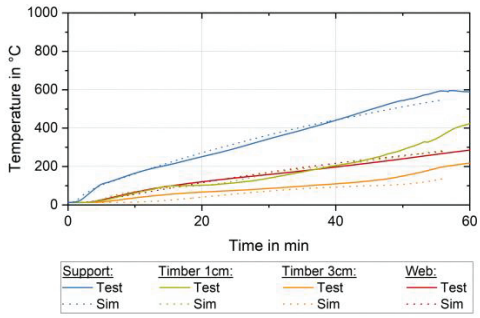

Figure 14: Comparison of simulation and results for reactive fire protection system with no backing

At the measurement point in the CLT element at a depth of 3 cm, more significant deviations are observed, as before. This is likely due to the test specimen's imperfections influencing the results. However, even during the experiments, significant fluctuations between the beams were observed despite identical setups, likely caused by uneven charring. For the specimen with a reactive fire protection system, the left section of the beam was constructed without a support layer, while the right section featured a narrow-side lining and a 12.5 mm support layer with gypsum plasterboards; the measurement curves were averaged separately for each beam side. Without the backing, good agreement was achieved at all measurement points (see Fig. 14). The influence of the intumescent fire protection coating with a 1.2 mm thick layer and the selected material parameters accurately represents the shielding effect caused by the expansion of the coating. Good approximations were also achieved for the area with the support layer and narrow-side lining. For the specimen with timber lining, the detachment of the lining was incorporated into the simulation based on previous validation tests. Two temperature thresholds were defined to align the simulation results with the measured values. When the average temperature of the bottom flange reached 150 °C, the furnace temperature was applied to the steel beam via convection to account for localized burn-throughs or deformations in the lining. Once the temperature reached 200 °C, the lining was completely removed by deleting the complete lining element from the simulation model, and the prevailing furnace temperature was applied as thermal exposure directly to the steel beam, combining radiation and convection effects. At the point where the lining detaches, a sharp increase in the temperature curve is observed. Using these temperature thresholds, the simulation produces a slightly conservative temperature profile (see Fig. 15).

6 – CONCLUSIONS

Fires in the support area and cavities of these systems are difficult to extinguish effectively. Mechanical load can lead to higher deformation if a charcoal layer has already formed. These challenges highlight the importance of implementing fire protection measures to prevent such situations.

https://doi.org/10.52202/080513-0449

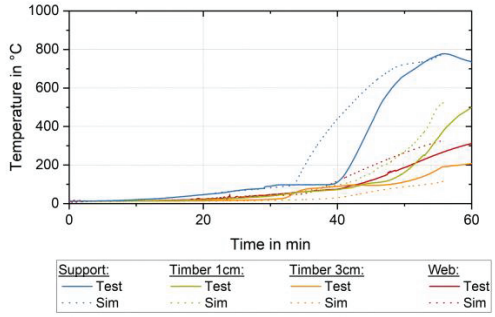

Figure 15: Comparison of simulation and results for specimen with timber lining

When using a 22 mm timber lining with one-sided fire exposure, the protective effect of the lining lasts for approximately 30 minutes. However, charring begins shortly after the lining detaches. It is recommended to use three-layer boards. Single-layer boards perform worse as increased charring occurs at the adhesive joints along the narrow sides.

With coatings, charring in the support area starts before the bottom flange of the steel beam reaches a critical temperature of 500 °C. Gypsum plasterboards used as backings can significantly delay the onset of charring by providing additional thermal protection, extending the time before critical temperatures are reached and delaying the charring of the CLT elements in the support area.

It should be noted that the intumescent fire protection coating results in lower thermal loads, causing the temperature in the support area to rise more slowly. The material parameters may be adjusted for the temperature-dependent shifts in specific heat capacity for scenarios involving a backing layer.

The influence of mechanical loading could not be demonstrated based on the temperature profiles recorded at the measurement points. Further experiments are recommended to verify whether adjustments to material properties are necessary to account for the increased charring rate observed under mechanical loading.

7 – PERSPECTIVE

Non-combustible panel materials were used to protect the support areas. Selecting appropriate fire protection materials that remain effective under compressive loads is essential. Further testing with additional materials is necessary to expand the database. Another possible approach is the active protection of the steel beam through fire protection coatings or fire-resistant hot-dip galvanisation. Optimisation concerning the char line of wood at 300 °C is conceivable and should be determined through experimental investigations.

Natural fire tests should be conducted to assess the charring behaviour of the floor during the cooling phase. The structural design should also ensure fire cannot penetrate the support area.

Recesses were made in the CLT elements to achieve a plane surface to accommodate the lining. However, the arrangement of the lamellae can lead to high transverse tensile stresses and wood splitting in the support area. Mechanically loaded tests would be helpful to optimise the load-bearing behaviour.

In the case of wide-flange beams and thick linings required for a 90-minute fire resistance rating, the increased span and weight could lead to premature detachment of the cladding and a reduction in the protection time. Further investigations should examine the suitability and influence of different fastener types and spacing.

8 – ACKNOWLEDGEMENTS

The IGF project number 22501 "Brandschutztechnisch sichere Konstruktionen in Stahl-Holz-Mischbauweise" of FOSTA is funded by the German Federal Ministry for Economic Affairs and Climate Action through Arbeitsgemeinschaft industrieller Forschungsvereinigungen (AiF) as part of the program to promote industrial collective research (IGF). This funding is provided based on a resolution of the German Bundestag.

9 – REFERENCES

[1] P. Dumler, J. Blankenhagen, N. Werther, S. Winter, M. Mensinger. "Validierungsversuche für brandschutztechnisch sichere Konstruktionen in Stahl-Holz-Mischbauweise." In: 9th Symposium Structural Fire Engineering (2023), pp. 19– 30.

[2] EN 1995-1-2, "Eurocode 5: Design of timber structures – Part 1-2: General – Structural fire design." Brussel, European Committee for Standardization, 2004.

[3] FprEN 1995-1-2, "Eurocode 5: Design of timber structures – Part 1-2: General – Structural fire design", Brussel, European Committee for Standardization, 2024.

[4] prEN 1991-1-2, "Eurocode 1: Actions on structures - Part 1-2: General actions - Actions on structures exposed to fire", Brussel, European Committee for Standardization, 2021.

[5] prEN 1993-1-2, "Eurocode 3: Design of steel structures - Part 1-2: General rules - Structural fire design", Brussel, European Committee for Standardization, 2022.

[6] V. Schleifer. "Zum Verhalten von raumabschliessenden mehrschichtigen Holzbauteilen im Brandfall." PhD thesis. ETH Zürich, 2009.

[7] A. Lucherini. "Fundamentals of thin intumescent coatings for the design of fire-safe structures." PhD thesis. University of Queensland, 2020.

[8] N. Bénichou, M. A. Sultan, C. MacCallum, J. Hum. "Thermal properties of wood, gypsum and insulation at elevated temperatures." National Research Council Canada, Institute for Research in Construction, Internal Report IR-710, Ottawa, 2001.

[9] J. R. Mehaffey, P. Cuerrier, G. Carisse. “A model for predicting heat transfer through gypsum-boards/woos-stud walls exposed to fire.” In: Fire and Materials, Vol. 18, pp. 297-305, 1994.

[10] J. Kolšek, P. Češarek. "Performance-based fire modelling of intumescent painted steel structures and comparison to EC3." In: Journal of Constructional Steel Research, Vol. 104, pp. 91-103, 2015.

[11] D. de Silva, A. Bilotta, E. Nigro. "Experimental investigation on steel elements protected with an intumescent coating." In: Construction and Building Materials, Vol. 205, pp. 232-244, 2019.

https://doi.org/10.52202/080513-0449